Published in final edited form as:
Nat Methods. 2009 February ; 6(2): 135–138. doi:10.1038/nmeth.1293.

Large-Scale Profiling of Protein Palmitoylation in Mammalian Cells

Brent R. Martin and **Benjamin F. Cravatt***
The Skaggs Institute of Chemical Biology and Department of Chemical Physiology, The Scripps Research Institute, 10550 N. Torrey Pines Rd., La Jolla, CA 92037

Abstract

S-palmitoylation is a pervasive post-translational modification required for the trafficking, compartmentalization, and membrane-tethering of many proteins. We demonstrate that the commercially available compound 17-octadecynoic acid (17-ODYA) can serve as a bioorthogonal, click chemistry probe for *in situ* labeling, identification, and verification of palmitoylated proteins in human cells. We identified ~125 predicted palmitoylated proteins, including G proteins, receptors, and a family of uncharacterized hydrolases whose plasma membrane localization depends on palmitoylation.

S-palmitoylation is a reversible covalent post-translational attachment of fatty acids on cysteines that mediates association of diverse proteins with membranes via a labile acyl-thioester linkage[1]. Many proteins have been identified as targets of palmitoylation, most notably G proteins, which are often palmitoylated proximal to prenylation or myristoylation sites. Other diverse classes of palmitoylated proteins include ion channels, receptors, cytoskeletal proteins, and kinases.

Protein palmitoylation has historically been detected by metabolic incorporation of radiolabeled palmitate followed by immunoprecipitation. This classical approach is tedious due to lengthy film exposure times and the lack of any straightforward means to enrich and identify radiolabeled proteins. Alternatively, selective thioester hydrolysis and covalent tagging can be used to capture sites of palmitoylation in a method termed acyl-biotin exchange (ABE)[2]. Coupling this approach to mass spectrometry provided the first global profile of palmitoylated proteins in *Saccharomyces cerevisiae*, identifying nearly 50 palmitoylation targets. The ABE method, however, requires complete blockage of all reduced cysteines to eliminate false-positives, as well as highly efficient thioester hydrolysis and disulfide-exchange reactions to label and identify palmitoylated proteins. Coupled with the inherent background observed with streptavidin bead enrichments, these factors have resulted in nearly 1/3 of the identified proteins being designated as false-positives[2]. Despite this initial promising work, large-scale identification of palmitoylated proteins from higher eukaryotic organisms, such as mammals, has yet to be reported, and we accordingly still lack an understanding of the full extent and purpose of this post-translational modification in cell biology.

Several groups have recently reported the use of azido-fatty acids or azido-acyl-CoAs as probes for protein myristoylation and/or palmitoylation[3–6]. Myristoylation describes the irreversible co-translational modification of the *N*-terminal residue (typically glycine) of proteins by myristoyl-CoA via an amide linkage. After reaction with biotin-linked phosphines by the Staudinger ligation, probe-modified proteins can be detected by avidin-HRP blotting. Each

*Correspondence should be addressed to B.F.C. (cravatt@scripps.edu).

report demonstrates the utility of this approach for rapid detection of acylated proteins, but stopped short of applying these probes for the global enrichment and identification of fatty acylated proteins from native biological systems.

Building on these past studies, we describe herein a simple and robust method for the global identification of palmitoylated proteins from human Jurkat T-cells using the commercially available compound 17-octadecynoic acid (17-ODYA)[7]. For decades, 17-ODYA has been used as a ω-hydroxylase inhibitor for *in vitro* and *in vivo* inhibition of cytochrome P450 metabolism of fatty acids. We now describe an additional application of 17-ODYA as a metabolically incorporated biorthogonal probe for profiling endogenous protein targets of palmitoylation (Fig. 1a). We detected octadecynoylated proteins via the Cu(I)-catalyzed azide-alkyne [3 + 2] cycloaddition reaction (click chemistry) to rhodamine-azide or biotin-azide reporter groups. Optimal metabolic labeling was observed following incubation with 25 μM of 17-ODYA for 6 or more hours (Supplementary Figs. 1 and 2), and labeled proteins were restricted to the membrane fraction (Supplementary Fig. 3). Nearly all detectable labeling was hydroxylamine-sensitive, signifying *S*-acylation is the predominant mode of protein modification by 17-ODYA (Fig. 1b).

To identify the targets of palmitoylation, membrane fractions from 17-ODYA-labeled Jurkat T-cells were reacted with biotin-azide and enriched for proteomic analysis by the multidimensional protein identification technology (MudPIT)[8] (Table 1). In our first study (n = 6 / group), 17-ODYA-treated cells were compared to cells treated with an equal concentration of palmitic acid. In a second study (n = 5 / group), cells were labeled with 17-ODYA, and half of the sample was treated with pH-neutral hydroxylamine to cleave 17-ODYA-protein thioester linkages. Protein levels in each sample were estimated by spectral counting, which sums the number of MS/MS spectra assigned to a specific protein and is highly correlated with protein abundance[9]. Stringent thresholds were applied to define predicted palmitoylated proteins as targets that appeared in either 17-ODYA dataset with: 1) an average spectral count value ≥ 5, 2) signal in at least three replicate samples, and 3) spectral count ratios of ≥ 5 for 17-ODYA-treated versus corresponding control samples (Supplementary Table 1). In total, these two datasets led to the classification of 125 high-confidence predicted palmitoylated proteins. Lowering the spectral count threshold to include proteins with an average spectral count value between 2 and 5 resulted in the identification of an additional ~200 predicted palmitoylated proteins, which we designated as medium-confidence targets (Supplementary Table 2).

Many of the predicted palmitoylated proteins are homologues of known palmitoylated proteins characterized in yeast, including 13 members of the multi-transmembrane solute carrier family of transporters, 11 SNAREs, and several metabolic enzymes[2]. The palmitoyl acyl-transferases (PATs) DHHC5, DHHC6, DHHC20, and HIP14 were also identified as targets of acylation, signifying either auto-palmitoylation or capture of palmitate-loaded catalytic intermediates. We further identified several known T-cell-specific targets of palmitoylation, including CD3, CD4, LAT, and LCK. In addition to these previously verified palmitoylated proteins, our data set contained many proteins for which no previous link to palmitoylation has been made.

Any large-scale MS-based profiling method is susceptible to generating false-positive data, which can become particularly problematic for interpretation of lower-abundance signals[10]. Accordingly, we sought to establish a robust protocol to quickly validate proteins enriched in 17-ODYA-treated samples. This method takes advantage of the fact that 17-ODYA-labeled proteins can be visualized by one of multiple platforms, including gel-based readouts (by click chemistry conjugation to fluorescent azide tags), which are much simpler and higher-throughput than LC-MS. 12 high-confidence and 6 medium-confidence targets were successfully over-expressed in 293T cells as determined by anti-FLAG western blot.

Membrane lysates of the 17-ODYA-labeled cells were directly labeled with rhodamine-azide and analyzed by SDS-PAGE. Shown in Supplementary Fig. 4 are results for a representative 15 of these 18 proteins. Of the 18 proteins analyzed, only two (PTBP1 and SHMT2) failed to show any evidence of palmitoylation in 293T cells. Thus, we were able to validate ~90% (16/18) of this set of novel acylation targets, including 11 of 12 high confidence hits and 5 of 6 medium-confidence hits, suggesting that our LC-MS profiles contain a low overall false-positive rate. The validated group also contained several potential *N*-myristoylation targets, including C11orf59, IGSF8, MREG, and PAFAH, based on the presence of an *N*-terminal Met-Gly sequence. PAFAH2 is a characterized target of myristoylation[11], and showed a hydroxylamine-resistant fluorescent band, as did C11orf59 (Supplementary Fig. 4). The other putative myristoylated proteins showed either complete or near-complete loss in signal following hydroxylamine treatment. These results argue that 17-ODYA can also be incorporated into endogenous sites of *N*-myristoylation. Since *N*-myristoyltransferases have exquisite selectivity for acyl-chains < C16 in length[12], we interpret our data to indicate that *N*-myristoylated proteins are likely labeled by metabolic products of 17-ODYA fatty acid oxidation, which is presumably the major route of probe degradation.

Included in our dataset were three members of a group of seven highly conserved (> 70%), uncharacterized human serine hydrolases, termed FAM108 proteins (Fig. 2a and Supplementary Fig. 5). We have previously shown these enzymes are exclusively found in the membrane fraction of the mouse brain proteome, where their activity was detected by activity-based protein profiling with serine hydrolase-reactive fluorophosphonate (FP) probes[13], such as FP-biotin and FP-rhodamine[14]. Interestingly, none of the FAM108 enzymes possess predicted transmembrane domains, suggesting that their exclusive presence in membrane proteomes is due to a distinct mechanism. Our data raised the possibility that these enzymes associate with the membrane via palmitoylation. The FAM108 protein family shares a highly conserved *N*-terminal stretch of 4–5 cysteines, which are candidate sites of palmitoylation (Fig. 2b). Consistent with this premise, *C*-terminal GFP fusion revealed striking plasma membrane localization for FAM108 proteins (Fig. 2c and Supplementary Fig. 5), which was eliminated by deletion of the *N*-terminal cysteine cluster (Fig. 2d). This truncation did not appear to impair enzyme activity, since each enzyme still reacted with FP-rhodamine[14]. In contrast, *N*-terminal-truncated FAM108 enzymes showed a complete loss of palmitoylation signals as judged by 17-ODYA labeling and a clear shift in subcellular distribution from the membrane/particulate to soluble proteome (Fig. 2e). Interestingly, FAM108C1, which contains one less *N*-terminal cysteine, exhibited significantly less 17-ODYA labeling and was more diffusely distributed and enriched on internal membranes (Supplementary Fig. 5). This finding suggests that multiple cysteines near the *N*-termini of FAM108 proteins are palmitoylated and the extent of palmitoylation could dictate the subcellular localization of these enzymes.

Understanding the complexities of protein acylation remains a major challenge. Here we report the first global inventory of acylated proteins from human cells using a bioorthogonal labeling strategy that exploits commercially available reagents (17-ODYA, reporter tagged-azides) for the enrichment and identification of palmitoylated proteins. We also provide a technically straightforward gel-based method to rapidly validate palmitoylated proteins identified by large-scale proteomic screens. Global proteomic analysis will be essential for identifying the specific targets of individual palmitoyl acyl transferases and thioesterases, and provide the tools to define the etiology of their related (patho)physiological functions. In contrast to static measurements like ABE, metabolic labeling with 17-ODYA can potentially allow for a more straightforward assessment of dynamic palmitoylation, by, for instance, following the time-course of acylation. Furthermore, given the literature precedent of using 17-ODYA *in vivo*[15], this probe may prove useful for profiling palmitoylation events in a range of organisms, including mammals.

Supplementary Material

Refer to Web version on PubMed Central for supplementary material.

Acknowledgments

We would like to thank Eranthie Weerapana for providing reagents and assistance with click chemistry and mass spectrometry, Gabriel Simon for assistance with data analysis, William Kiossis for microscopy instruction, and members of the Cravatt lab for helpful discussions. This research was funded by F32NS060559, CA087660, and the Skaggs Institute for Chemical Biology.

References

1. Linder ME, Deschenes RJ. Nat Rev Mol Cell Biol 2007;8(1):74–84. [PubMed: 17183362]
2. Roth AF, et al. Cell 2006;125(5):1003–1013. [PubMed: 16751107]
3. Hang HC, et al. J Am Chem Soc 2007;129(10):2744–2745. [PubMed: 17305342]
4. Heal WP, et al. Chem Commun (Camb) 2008;(4):480–482. [PubMed: 18188474]
5. Kostiuk MA, et al. FASEB J 2008;22(3):721–732. [PubMed: 17971398]
6. Martin DD, et al. FASEB J 2008;22(3):797–806. [PubMed: 17932026]
7. Shak S, Reich NO, Goldstein IM, Ortiz de Montellano PR. J Biol Chem 1985;260(24):13023–13028. [PubMed: 2997155]
8. Link AJ, et al. Nat Biotechnol 1999;17(7):676–682. [PubMed: 10404161]
9. Old WM, et al. Mol Cell Proteomics 2005;4(10):1487–1502. [PubMed: 15979981]
10. Elias JE, Gygi SP. Nat Meth 2007;4(3):207–214.
11. Matsuzawa A, et al. J. Biol. Chem 1997;272(51):32315–32320. [PubMed: 9405438]
12. Towler DA, et al. J Biol Chem 1988;263(4):1784–1790. [PubMed: 3123478]
13. Blankman JL, Simon GM, Cravatt BF. Chem Biol 2007;14(12):1347–1356. [PubMed: 18096503]
14. Liu Y, Patricelli MP, Cravatt BF. Proceedings of the National Academy of Sciences of the United States of America 1999;96(26):14694–14699. [PubMed: 10611275]
15. Gebremedhin D, et al. J Vasc Res 1993;30(1):53–60. [PubMed: 8435472]

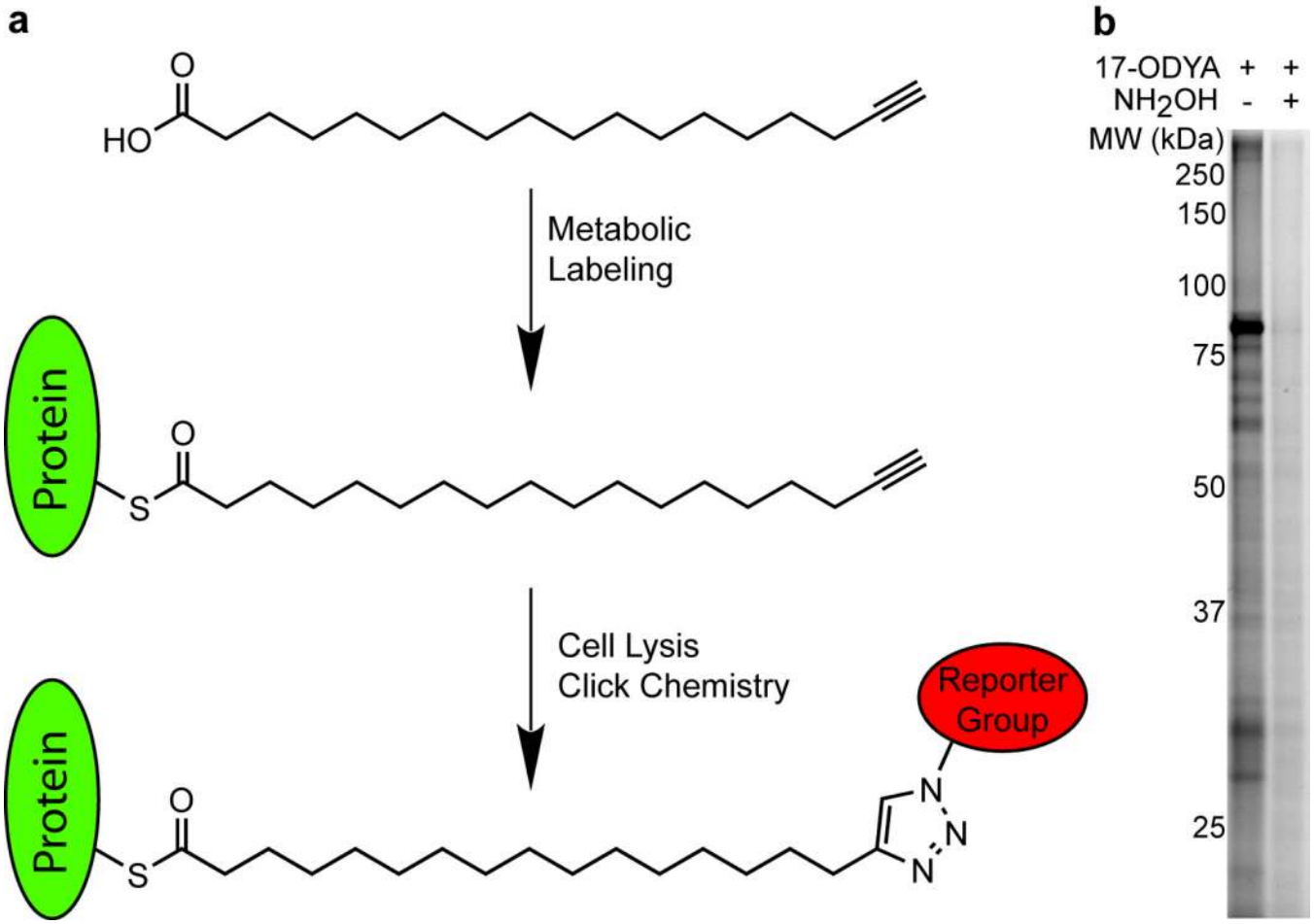

Figure 1.

17-ODYA labeling and detection of palmitoylated proteins. (**a**) Schematic of 17-ODYA labeling. Cultured Jurkat T-cells were metabolically labeled with 17-ODYA and the lysates were then reacted with rhodamine-azide or biotin-azide for gel-based and LC-MS-based characterization of palmitoylated proteins. (**b**) Profiling palmitoylated proteins in the membrane fraction of Jurkat T-cells incubated with 25 μM 17-ODYA for 8 hours. Half of the sample was boiled in 2.5% hydroxylamine (NH_2OH) for 5 minutes to hydrolyze thioesters and remove 17-ODYA labeling.

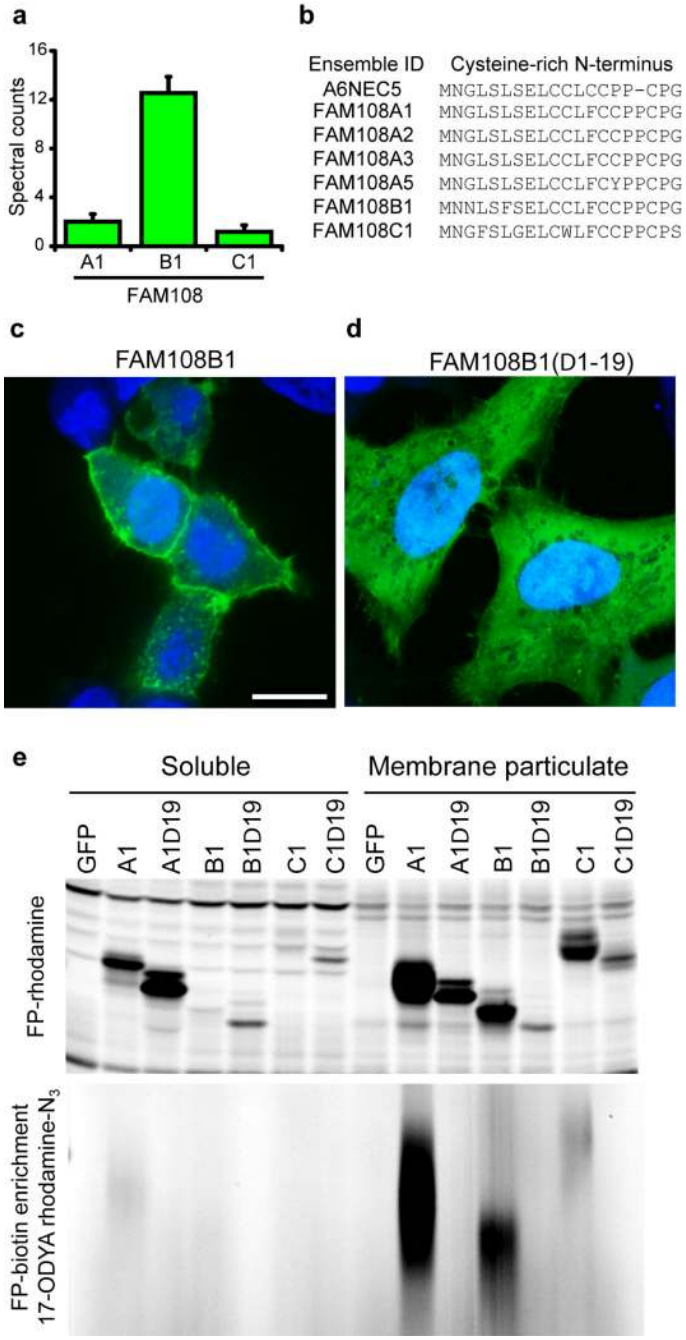

Figure 2.

Membrane tethering of the FAM108 family of serine hydrolases by palmitoylation of an *N*-terminal cysteine-rich motif. (**a**)Average spectral counts of three FAM108 proteins identified by 17-ODYA profiling of Jurkat T-cells. None of these proteins showed any spectral counts in either the palmitate or hydroxylamine controls. (**b**) Cysteine-rich amino acid motif conserved among the seven members of the FAM108 family of proteins. FAM108A3 and FAM108A5 (which were not identified in this study) contain an additional N-terminal sequence preceding the cysteine-rich region of 73 and 28 amino acids respectively. (**c**) Distribution of FAM108B1-GFP fusion protein (green) expressed in HeLa cells co-stained with DAPI (blue). Scale bar = 15 μm. (**d**) Distribution of FAM108B1(Δ1–19)-GFP (green) expressed in HeLa cells co-

stained with DAPI (blue). Deletion of the *N*-terminal cysteine-rich domain prevents FAM108B1 from localizing to the plasma membrane. (**e**) The N-terminal cysteine-rich motif of FAM108 proteins is palmitoylated and responsible FAM108 membrane localization. FAM108 proteins are fluorophosphonate (FP)-reactive serine hydrolases, which can be efficiently labeled with activity-based probes such as FP-rhodamine or FP-biotin[14]. The upper panel shows FP-rhodamine-labeled soluble and membrane particulate fractions. The distribution of active FAM108 protein is altered from the particulate to soluble fractions by deletion of the *N*-terminal cysteine-rich motif. In the lower panel, 17-ODYA labeled transfected 293T cells were labeled with FP-biotin and enriched with streptavidin-agarose beads, reacted with rhodamine-azide, and visualized by in-gel fluorescence scanning.

Table 1

Spectral counts for the top 35 high-confidence palmitoylated proteins. Proteins are listed according to highest total spectral counts identified in both Experiment #1 and Experiment #2, which compare 17-ODYA labeled membrane particulate proteomes to palmitic acid-treated and hydroxylamine–treated controls, respectively. Proteins with a consensus myristoylation site (*N*-Met-Gly) are colored in red. Spectral count data represents average values ± standard errors.

Ensemble ID	Protein Name	Experiment 1 (N = 6)		Experiment 2 (N=5)	
		17-ODYA	Palmitate	17-ODYA	Hydroxylamine
CANX	Calnexin	95 ± 11	11 ± 2	122 ± 30	2 ± 1
HLA-A;HLA-B;HLA-C	HLA class I histocompatibility antigen	68 ± 10	13 ± 6	68 ± 12	0 ± 0
LCK	Proto-oncogene tyrosine-protein kinase LCK	75 ± 13	1 ± 1	25 ± 4	4 ± 1
TXNDC1	Thioredoxin domain-containing protein 1	63 ± 9	0 ± 0	31 ± 5	2 ± 1
MTDH	Metadherin / LYRIC	45 ± 8	0 ± 0	42 ± 4	1 ± 1
CD3D	T-cell surface glycoprotein CD3 delta chain	29 ± 7	0 ± 0	48 ± 14	1 ± 1
SCAMP3	Uncharacterized protein SCAMP3	21 ± 3	3 ± 1	58 ± 28	4 ± 0
SNAP23	Synaptosomal-associated protein 23	25 ± 3	2 ± 1	44 ± 16	0 ± 0
RAP2B	Ras-related protein Rap-2b	37 ± 3	0 ± 0	26 ± 4	0 ± 0
GNAQ	Guanine nucleotide binding protein q subunit	38 ± 8	0 ± 0	23 ± 2	0 ± 0
KIAA0152	Uncharacterized protein KIAA0152	34 ± 8	0 ± 0	21 ± 4	0 ± 0
PI4K2A	Phosphatidylinositol 4-kinase type 2-alpha	30 ± 4	0 ± 0	20 ± 2	0 ± 0
RAP2C	Ras-related protein Rap-2c precursor	34 ± 2	0 ± 0	12 ± 2	0 ± 0
FLOT1	Flotillin-1	24 ± 5	0 ± 0	19 ± 4	0 ± 0
RAP2A	Ras-related protein Rap-2a	22 ± 2	0 ± 0	9 ± 2	0 ± 0
SYBL1	Synaptobrevin-like protein 1	12 ± 1	0 ± 0	18 ± 4	0 ± 0
GNA13	Guanine nucleotide-binding protein alpha-13 subunit	18 ± 3	0 ± 0	9 ± 1	0 ± 0
IGSF8	Immunoglobulin superfamily member 8	11 ± 1	0 ± 0	16 ± 2	0 ± 0
EBAG9	Placenta derived apoptotic factor	10 ± 3	0 ± 0	17 ± 2	0 ± 0
AGPAT1	1-acyl-sn-glycerol-3-phosphate acyltransferase alpha	17 ± 4	0 ± 0	8 ± 2	0 ± 0
FAM62B	Uncharacterized Protein FAM62B	16 ± 4	0 ± 0	8 ± 2	2 ± 1
FAM108B1	Uncharacterized abhydrolase domain-containing protein	15 ± 1	0 ± 0	10 ± 2	0 ± 0
VANGL1	Vang-like protein 1	13 ± 1	0 ± 0	11 ± 1	0 ± 0
SCAMP2	Secretory carrier-associated membrane protein 2	8 ± 1	0 ± 0	16 ± 1	0 ± 0
LNPEP	Isoform 1 of Leucyl-cystinyl aminopeptidase	15 ± 3	0 ± 0	7 ± 3	0 ± 0
BAT5	Uncharacterized abhydrolase domain-containing protein	11 ± 2	0 ± 0	11 ± 3	0 ± 0
STX12	Syntaxin-12	10 ± 2	0 ± 0	13 ± 1	0 ± 0
SCAMP1	Secretory carrier-associated membrane protein 1	9 ± 1	0 ± 0	10 ± 2	0 ± 0
RHBDD2	Rhomboid domain-containing protein 2	14 ± 4	0 ± 0	3 ± 1	0 ± 0
HMOX2	Heme oxygenase 2	9 ± 1	0 ± 0	9 ± 1	0 ± 0
HADHB	Trifunctional enzyme beta subunit	11 ± 2	0 ± 0	7 ± 1	0 ± 0
GNA11	Guanine nucleotide-binding protein subunit alpha-11	14 ± 2	0 ± 0	4 ± 3	0 ± 0
STX8	Syntaxin-8	9 ± 2	0 ± 0	9 ± 3	0 ± 0
ZDHHC20	Probable palmitoyltransferase ZDHHC20	5 ± 1	0 ± 0	14 ± 6	0 ± 0
SLC1A5	Neutral amino acid transporter B	10 ± 2	1 ± 1	7 ± 2	0 ± 0